FIELD TEST AND 3D FE MODELING OF DECKED BULB-TEE BRIDGES

Z. (John) Ma, Ph.D, PE, Dept. of Civil & Envir. Eng., University of Alaska Fairbanks
Jason L Millam, Dept. of Civil & Envir. Eng., University of Alaska Fairbanks
Sanjay Chaudhury, Dept. of Civil & Envir. Eng., University of Alaska Fairbanks
J. Leroy Hulsey, Ph.D, PE, Dept. of Civil & Envir. Eng., University of Alaska Fairbanks
Elmer Marx, PE, Bridge Design, Alaska Department of Transportation, Alaska

ABSTRACT

This paper summarizes field-testing of 8 decked bulb-tee girder bridges as well as development of 3D finite element and 2D grillage models. Based on field tests and bridge model analysis, single-lane live-load distribution factors (DFs) for both shear and moment are presented in the paper. These DFs are compared with current AASHTO Specifications. Based on analyzed data, the moment DF values from AASHTO LRFD are an average of 66% larger than the experimentally derived values and the shear DF values from AASHTO LRFD are an average of 26% larger than the experimental values. The analyzed data is much more closely approximated by the single lane DF equations in AASHTO LRFD Specifications reserved for decked bulb-tee girder bridge systems that have transverse post-tensioning to act as a single unit. The developed 3D FE model and 2D grillage model work well in predicting the single lane live load distribution factors. The calibrated 3D FE model can be used to study the shear connectors in decked bulb-tee bridges. The stiffness modeling of the transverse beams play a significant role in the accuracy of the grillage models. Grillage models show that concrete strengths have no impact on DF values.

Keywords: Single Lane, Load Distribution, Bridges, Load Rating, Field Test, 3D Finite Elements, Grillage, AASHTO Specifications, Decked Bulb-Tee, Shear Connectors, Intermediate Steel Diaphragms, High Strength Concrete.

INTRODUCTION

The Alaska Department of Transportation and Public Facilities (AKDOT&PF) uses AASHTO Load Resistance Factor Design (LRFD) Bridge Design Specifications[1] for design and evaluation of Alaska's highway bridges. Most of the new bridges in the state are constructed from the Alaska decked bulb-tee girder. Because there is a longitudinal joint (hinge) between girders for this type of bridge, AASHTO lists this bridge under a different category when calculating live load distribution factors (DFs). According to the current AASHTO LRFD Specifications, there are two different live load DF equations for bulb-tee girder bridges other than the Alaska decked bulb-tee type. One equation is for single lane loaded, and the other for two or more lane loaded. For the Alaska decked bulb-tee bridges, however, the AASHTO LRFD Specifications only provide for one live load DF equation. That equation was based on data from two or more lane loaded bridges[2]. Reference 2 also documented the historical development[3, 4] of that equation in both AASHTO Standard Specifications[5] and AASHTO LRFD Specifications. It has been concluded in Reference 2 that similar to other slab-and-beam bridge systems, a single lane loaded DF formula for Alaska style decked bulb tee bridges should be specified in the AASHTO Specifications to consider the impact of loaded lanes on calculation of DF. A single lane loaded DF formula is also needed in load rating bridges.

Load ratings are used to limit the vehicle load that may legally cross the bridge. Many older bridges in Alaska, designed to lesser load requirements, are found to have substandard load ratings. For example, in many cases the shear load ratings for older prestressed concrete girders control the load limit for the bridge. To increase the shear rating for these older bulb-tee bridges, one method is to field measure the fraction of an applied live load that is transferred to a single girder. Live load distribution factors are used to express how a load applied to the bridge is shared between adjacent girders. Subsequently, a study was funded by AKDOT&PF to develop a single lane distribution factor equation for Alaska decked bulb-tee girder bridges.

FIELD TESTING PROGRAM

Field loading testing generally gives a realistic determination of the live load distribution. Most of tests were conducted on beam-and-slab bridges. The most extensive single effort of field testing was conducted at the AASHO Test Road[6]. However, only three full-scale tests of the type of multi-beam bridges studied have been reported[7, 8, 9]: The first test[7] was conducted on a bridge consisting of channel sections; the second[8] was on a bridge with solid sections with holes; and the third[9] test was on a bridge composed of solid sections.

In order to determine single-lane load distribution factors for decked bulb-tee bridges, a field testing program has been developed under the current research project at the University of Alaska Fairbanks (UAF). In selecting the test bridges, UAF researchers considered the following factors. (1) They are all located in or near Anchorage, Alaska. (2) Traffic can be closed during late night hours for all these bridges. (3) They are all accessible to instrument. And (4) they represent different geometry of the bridges in Alaska in terms of skew angles and aspect ratio (length/width). Researchers have also decided to test paired structures to provide verification of the instrumentation and modeling procedures. Based on these factors, four pairs (Sets 1, 2, 3, and 4) of bridges have been identified and tested, as shown in Table 1.

Table 1 Field Tested Bridges (From May 6 to May 19, 2003)

Name		Bridge Geometry			Girder	
		Span(ft)	Width(ft)	Skew(^{o})	Spacing(in.)	Depth(in.)
Set 1	W100th NB	116.0	37.0	0	88.4	54.0
	W100th SB					
Set 2*	Dimond Rd	110.0	107.0	0	90.6	54.0
	Dowling Rd					
Set 3	Campbell NB	139.0	37.0	4.3	88.4	65.0
	Campbell SB					
Set 4	Huffman NB	128.0	37.0	27.5	72.0	54.5
	Huffman SB					

** Note: Tee shape girder in Set 2 instead of decked Bulb-Tee shape used in Set 1, 3, and 4.*

In the field bridge tests, full-bridge reusable strain transducers fabricated by Bridge Diagnostics, Inc. (BDI) were used. Transducers were attached to the concrete using Loctite Brand instant adhesive. Strain values were collected through the Data Acquisition System – MEGADAC 5414 Series by former OPTIM Electronics. This system was connected to a laptop computer utilizing TCS for Windows Version 3.4 Software, as shown in Figure 1. The gauges were placed in areas that experience the largest stresses in the bridge.

LOAD VEHICLE DESCRIPTION AND POSITIONING

Loaded AKDOT&PF end dump truck was used as loading vehicle. Figure 2 shows the approximate vehicle foot-print location and wheel loads. Wheel loads were measured on May 8, 2003 with a measured error of ± 1%.

Fig. 1 Movable Field Testing "Lab"

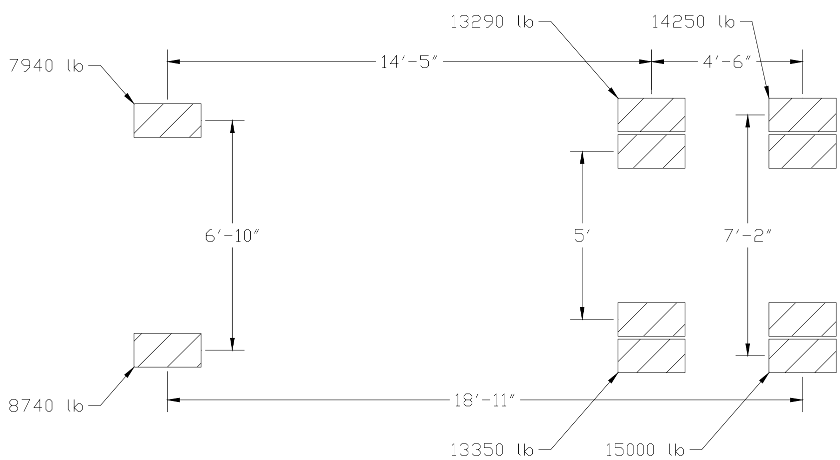

Fig. 2 Load Vehicle Measurement

During loading, the load vehicle would travel across the bridge in the same direction for each transverse load position, and for each loading condition. During the testing period, there were two main methods of loading the bridge: Continuous Loading and Static Loading. During Continuous Loading, as shown in Figure 3, the load vehicle was driven at a constant speed of two miles per hour along a straight longitudinal girder line across the bridge. Data during this loading condition recorded continuously before the load vehicle moved onto the bridge, while the vehicle moved across the bridge, and as the vehicle moved off the bridge. During this loading condition the transverse position of the vehicle is known, there is no method of relating the measured strain values to the vehicle's longitudinal position on the bridge. Normally, this loading condition was conducted to verify the accuracy of the data and determine whether or not any strain gauges might be malfunctioning. This loading condition can also be used to identify the maximum strains of the gauges, and thus the maximum distribution factors.

During the Static Loading, the load vehicle was driven to three known longitudinal stop positions along a given girder line. The first set of data was recorded as the vehicle was driven onto the bridge to its first stop position. The next set of data was recorded as the vehicle drove from its first stop position to its second stop position. The third set of data was recorded as the vehicle drove from its second stop position to its third stop position located roughly halfway along the length of the bridge. This loading method can be used to calibrate the bridge analytical models.

Fig. 3 Continuous Loading Test

Three data sets were recorded for each girder line or transverse positioning which the vehicle drove along. Figure 4 depicts the three longitudinal stop positions which the load vehicle moved to during the static loading condition. The first stop position places the vehicle with its driver's side rear wheel centered at a distance H (representing the girder depth) away from the abutment. The second stop positions locates the vehicle with its second axle (driver's side wheel) ¼ of the span length of the bridge. The third stop position locates the vehicle's second axle (driver's side wheel) at the center line of the bridge span. For non skew bridges, both the driver's side and passenger's side wheels will be located at the same relative longitudinal position.

The transverse loading positions are defined by the girder number over which they drive. The girder numbering system is as follows: Girder number one (G1) is always the furthest girder to the right of the bridge based off the direction of traffic, not the direction of loading, girders are then numbered consecutively from right to left. For most of the interior girders loaded, the load vehicle is positioned so that its wheels are centered over the centerline of the girder. For each exterior girder loaded, the vehicle is positioned with the centerline of its outside wheel line to be approximately 2 ft from the edge of the bridge. Figure 5 shows the wheel loads relative to the girders.

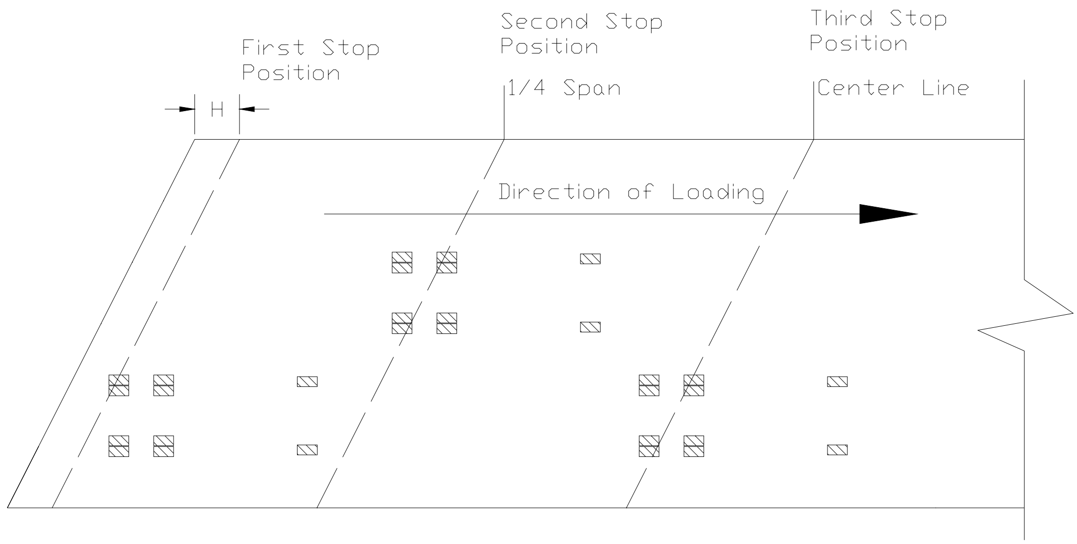

Note: The diagram depicts the vehicle at different transverse positions for clarity. During actual loading the vehicle stayed in the same transverse position as it moved to its three longitudinal stop positions.

Fig. 4 Longitudinal Vehicle Stop Positions

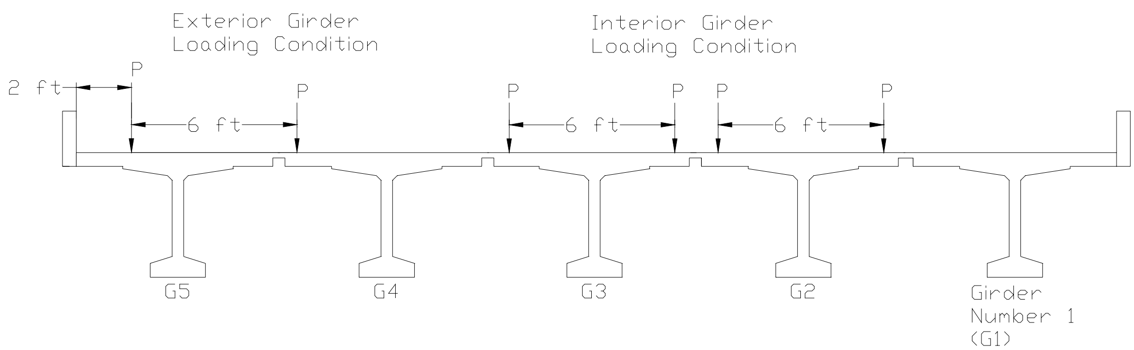

Fig. 5 Transverse Vehicle Positions (General)

STRAIN GAUGE POSITIONING

During field testing 24 gauges were placed to measure strains on each bridge. There were three main categories of gauge placement: one set of gauges would be used to measure shear response; the second set of gauges would be used to measure flexural stresses due to midspan moment; and the third set of gauges would be used to measure axial stress in the intermediate steel diaphragms.

For each girder, there were a potential of six different locations which we could place the shear gauges and two different locations which we could place the moment gauges. The shear gauges would always be placed a distance H (H = depth of the girder) away from the face of the end diaphragm and vertically on the approximate location of the neutral axis (N.

A.). The shear gauges could either be oriented 45deg towards (S1) or away (S3) from the end diaphragm or vertically (S2), as shown in Figures 6 and 7. They could also be positioned either on the right (S1R) or left (S1L) side of the girder. Note that the right and left hand side of a girder is distinguished by the direction in which the girder is loaded. The moment gauges were always positioned at midspan and located either centered on the bottom flange (M1) or on the left hand side of the web (M2). The moment gauges positioned on the web were located vertically at the highest position on the web just below the top flange. The positions of the gauges are shown in Figure 6. The right or left side of the girder is always based off of the direction the load vehicle moves across the bridge.

The Diaphragm gauges are located at either quarter span or midspan. The gauges were placed halfway between the midpoint of the K brace and the edge of the girder. The gauges are identified by the two girder between which they reside. Figure 8 shows the general location of the gauges on the steel diaphragms.

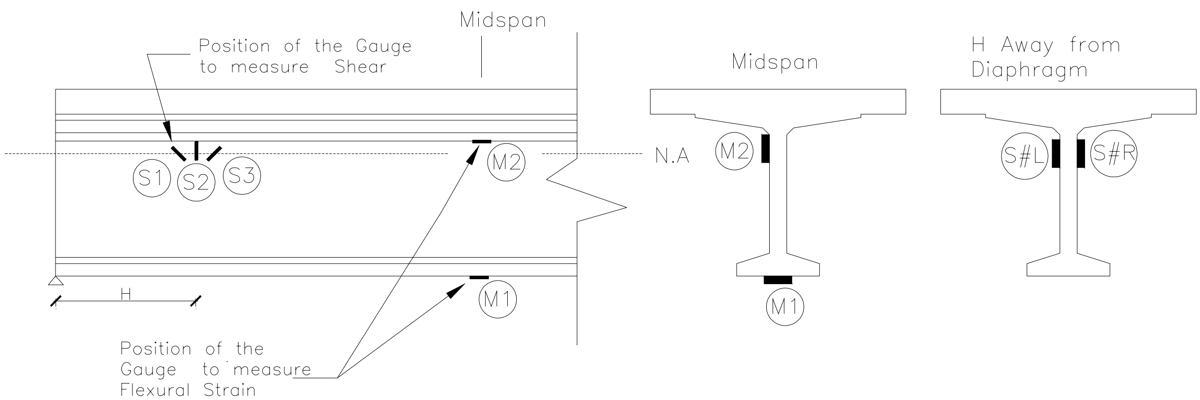

Fig. 6 Gauge Positions (Elevation)

Fig. 7 Three Shear Gauges

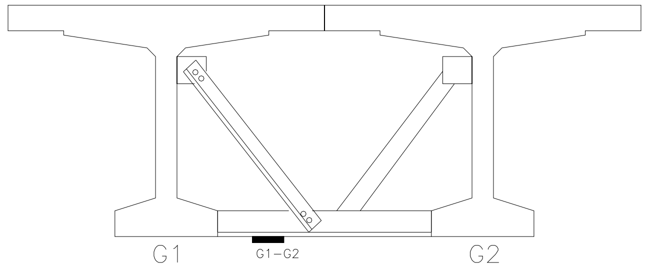

Fig. 8 Gauge Location on Steel Diaphragm

FIELD TESTING RESULTS

Using the data acquisition system, the data plots in Figures 9, 10, and 11 show the total strain vs. time. For the Static Loading method, the vehicle position is known. In the case of the Continuous Loading, it is possible to detect the approximate location the load vehicle is on the bridge. Take the W100th NB Bridge as an example. Figure 9 shows all of the gauges in S1 Position (angled 45deg into the end diaphragm, as shown in Figure 6) under the Continuous Loading. Since all of the gauges are in the same position, they are only distinguished by the girder number they are on and whether they are on the left (L) or right (R) side of that girder. For example, series G3R represents the shear gauge located on girder number 3 which is the middle girder of the W100th NB bridge, it is angled into the diaphragm and is on the right side of the girder.

Figure 10 shows the strains in the steel diaphragm of which only three gauges were placed on the steel diaphragms under the Continuous Loading. Each series is labeled by the two girders between which the diaphragm resides. Series G1-G2 M represents the strain gauge located on the steel diaphragm between girder's 1 and 2, and the M show that its location is at midspan instead of quarter span.

Figure 11 shows all of the midspan moment gauges under the Static Loading method. Each gauge is located at the bottom flange at the M1 position from Figure 6. For W100th NB there were no gauges placed in the M2 Position. Each of the different series represents the midspan gauge for a certain girder. For example, the series entitled G1 represents the gauge located at the M1 position on Girder number 1 which is an edge girder located on the right hand side of the W100th NB Bridge. Figure 11 also shows the all three vehicle stop positions for a given girder line.

Fig. 9 Strains at Position "S1" vs. Time (Vehicle Position)

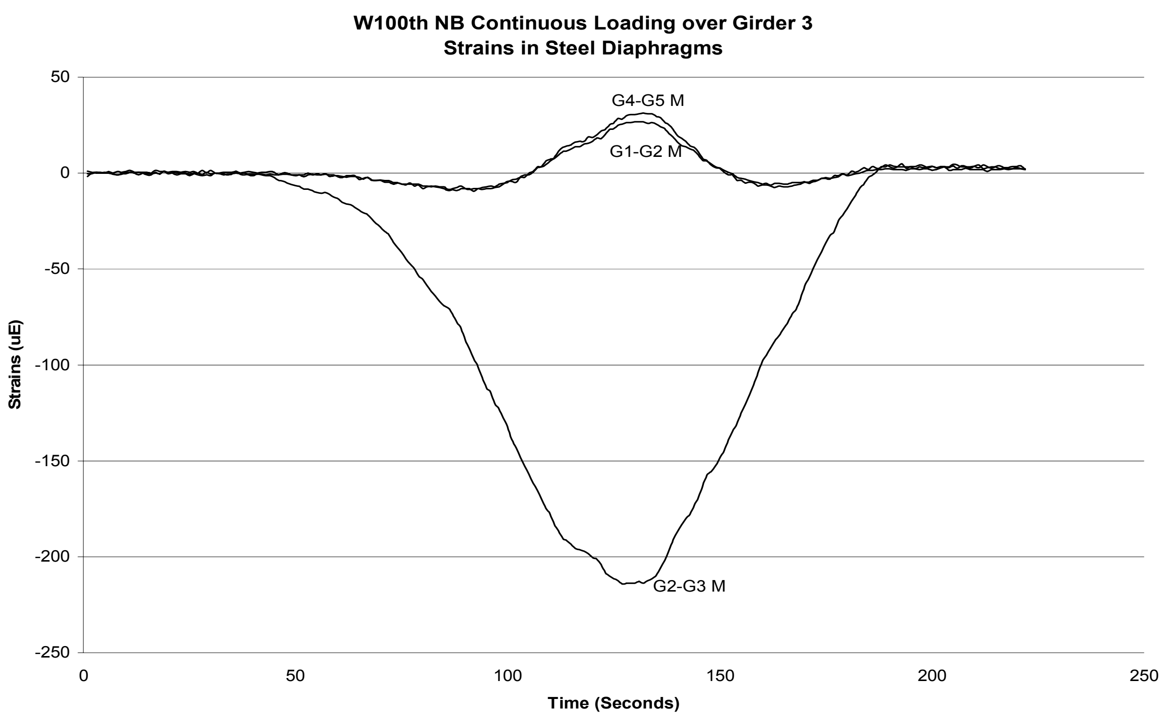

Fig. 10 Steel Diaphragm Strains vs. Time (Vehicle Position)

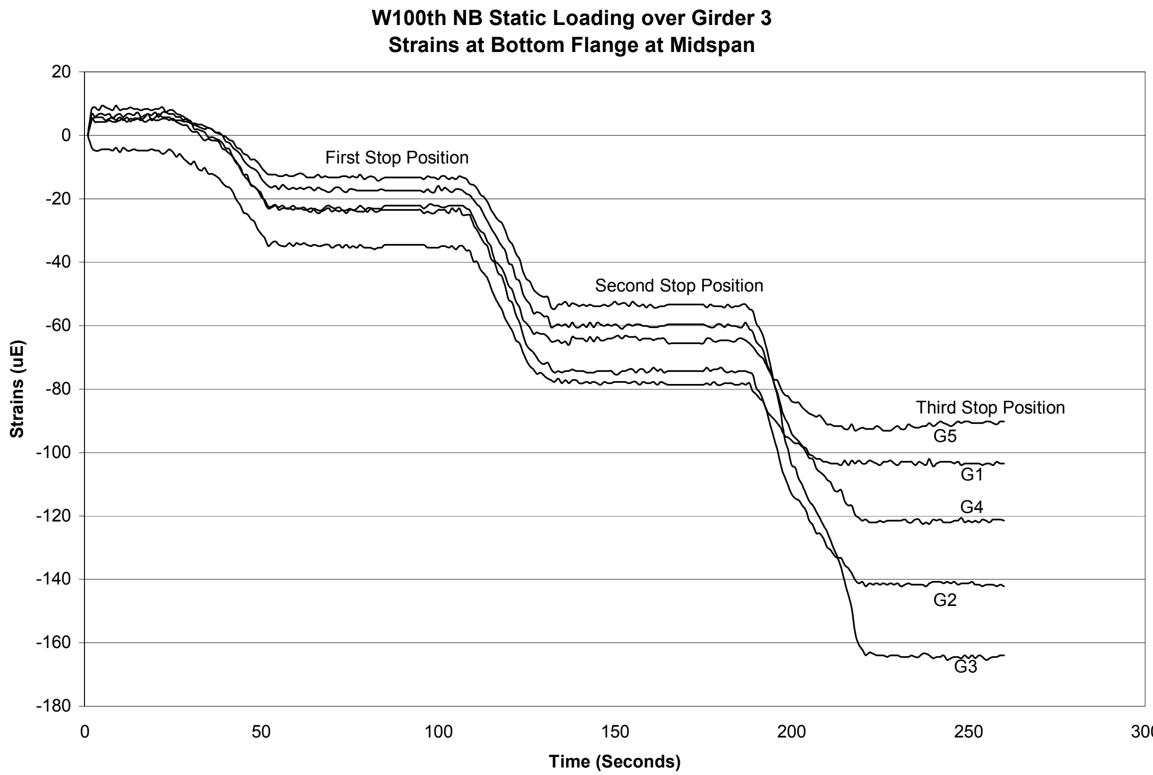

Fig. 11 Strains at "M1" Position vs. Time (Vehicle Position)

BRIDGE MODELING

One of the research objectives is to develop analytical models to analyze the behavior of the Alaska decked bulb-tee girder bridges. When developing load distribution factors for AASHTO LRFD Specifications, three levels of analysis were used[10]. Similar to this approach, the 3D finite element modeling and 2D grillage modeling were developed.

3D FINITE ELEMENT MODELING

The finite element (FE) method offers an improvement over most other methods. A three-dimensional (3D) model can accommodate interaction between girders, decks, shear connector joints, intermediate steel diaphragms and supports. This type of model treats the bridge deck as a three-dimensional system. Bearings are placed at actual locations the model. Each girder cross section may be modeled using a different mesh density. The mesh density is based on the location of the girder relative to the loading position. Methods of construction and different types of highway loading may also be studied by this method[11, 12].

Elements and Mesh

The 3D FE modeling was done by using ABAQUS Version 6.3 software available at the Arctic Region Supercomputing Center at UAF (http://www.arsc.edu). ABAQUS Version 6.3 contains a library of solid elements for three dimensional applications. The library of solid elements in ABAQUS contains first and second order isoparametric elements. These isoparametric elements are generally referred for most cases because they are usually the most cost effective of the elements that are provided in the ABAQUS. The 20-node brick element, as shown in Figure 12, has been used to model the bulb-tee girders for its improved inter-element compatibility.

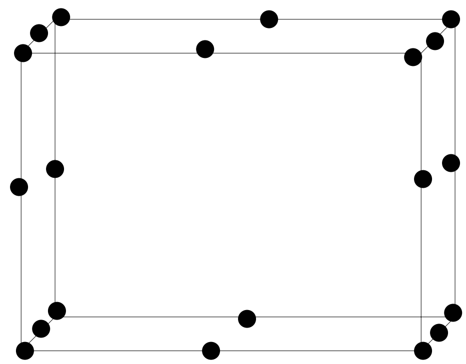

Fig. 12 The 20-node Solid Element

Between decked bulb-tee girders, there are two types of connections: shear connectors and intermediate steel diaphragms. The spacing of the connectors is 4 ft throughout the entire length of the structure. They were made of steel angles welded together by ¼" thick steel plates through the girder's top flange. These angles, 6 inches long in the longitudinal traffic direction, are embedded into the girder concrete through #4 steel bars. The intermediate steel diaphragms are also made of steel angles, as shown in Figure 8. In the 3D FE model, 2-node hinge-connector elements were used to model shear connectors. And 3D truss elements were used to model the intermediate steel diaphragms, as shown in Figure 13.

A sufficiently refined mesh was used to ensure that the results from ABAQUS simulation are adequate. Figure 14 shows one example of the refined mesh.

Boundary Conditions

The modeling has been done by taking the following assumptions. One end of the bride is assumed to be a roller support by restraining the bottom flange at the girder's end section in the vertical direction and in the transverse direction. The other end of the bridge is assumed to be a pin support by restraining all three directions. In modeling end diaphragms, two end sections of the girder are restrained in the transverse direction.

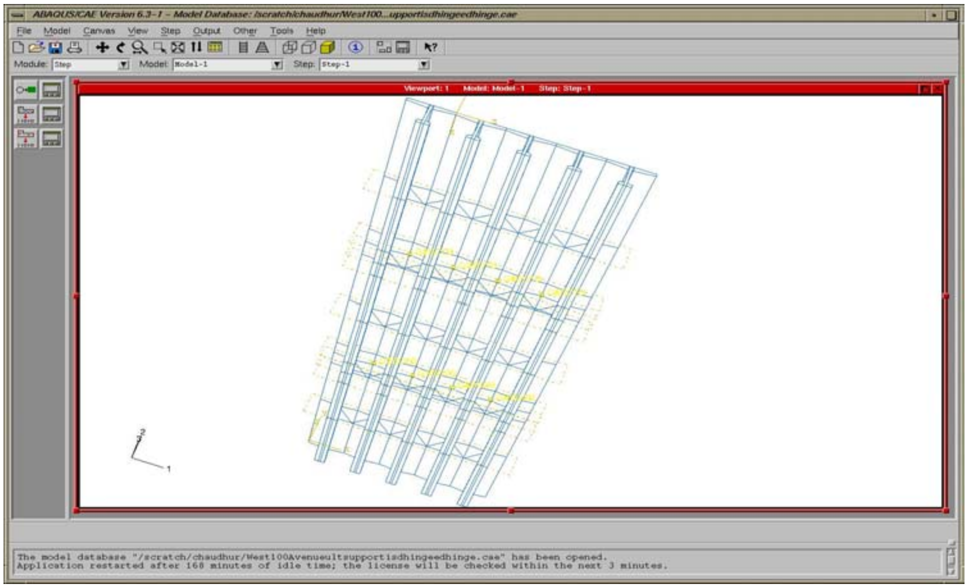

Fig. 13 Modeling Intermediate Steel Diaphragms

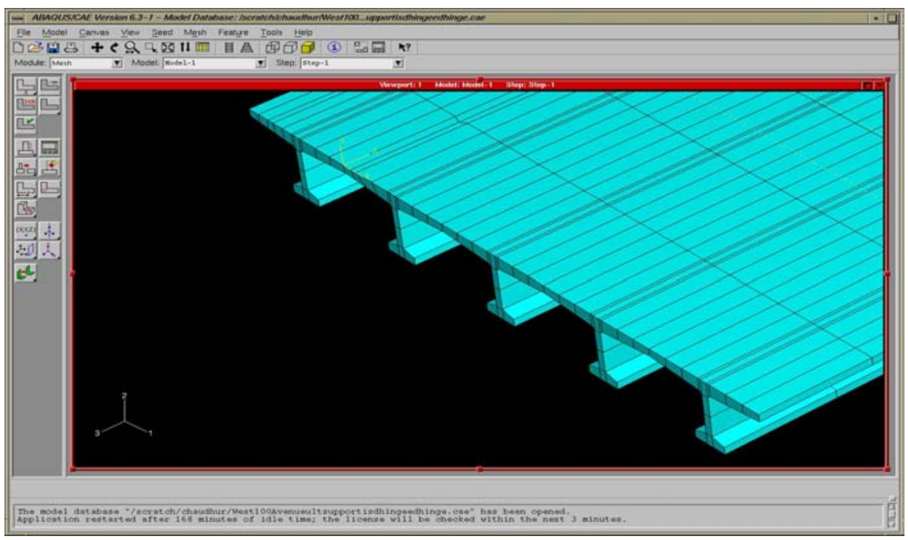

Fig. 14 Refined Mesh Example

2D GRILLAGE MODELING

A grillage analogy of the W100 NB bridge is shown in Figure 15. The grillage model has 5 longitudinal beams representing the 5 girders of the bridge. Each beam has the same moment of inertia as the decked bulb-tee girders they represent. Saint-Venant's torsional stiffness constant of the longitudinal beams was approximated using the current method described in the AASHTO LRFD Specifications for stocky open sections:

$$J = \frac{A^4}{40in \cdot I_p}$$

where A is the area of the Girder and I_p is the polar moment of inertia. We compared other methods of determining J such as the standard grillage approximation of adding the Horizontal and Vertical moments of inertia together, yet the AASHTO LRFD method produced results that most closely matched the testing data.

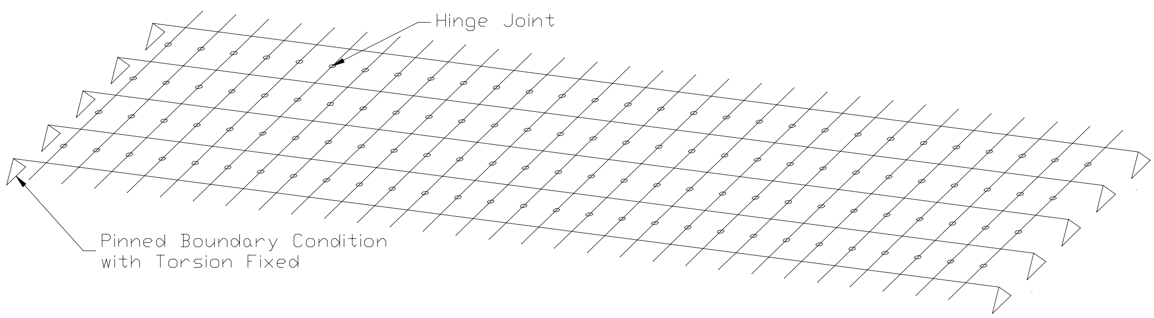

Fig. 15 Grillage Model of W100 NB Bridge

The transverse stiffness of the bridge deck is approximated by 29 beam lines each separated by 3.8 ft. We also varied the number of transverse beams and found that increasing the density of the grillage mesh had little impact on the distribution factor. The actual depth of the deck varies from 10” to 6” the largest transverse moment in the deck occurs directly over web section. Two grillage models are developed. In the first model (Grillage Model 1), the transverse beams are represented by a solid rectangular section that is 10” deep and 3.8 ft wide, while the second model (Grillage Model 2) uses 6” deep and 3.8 ft wide transverse beams. We also approximated the effects of the shear key located between each girder by placing a hinge joint on the transverse beams halfway between each girder in both models.

SINGLE LANE LIVE LOAD DISTRIBUTION FACTORS

Of the eight different bridges tested, the pair located at the intersection of W100th Ave. and Minnesota are the most standard of the eight bridges in that they have no skew have an average span length and width and are built with typical decked bulb-tee girders. Therefore, we will use the results from this pair of bridges as an example to discuss single lane live load distribution factors. In the figures below, the series entitled “NB” or “SB” stand for the data collected from either the North Bound bridge or the South Bound bridge. The series entitled “Stat” or “Cont” represent the Static Loading method or Continuous Loading method.

We calculated the single lane load distribution factor for moment by using the following method:

$$DF_{moment} = \frac{\varepsilon_x}{\varepsilon_1 + \varepsilon_2 + \varepsilon_3 + \varepsilon_4 + \varepsilon_5}$$

where ε_x is the strain measured directly under the loaded girder from the strain gauge at position "M1"; and ε_1 to ε_5 is the strain measured from all five gauges at position "M1" on each girder. The single lane distribution factor for shear was calculated in a similar method except each of the girder strains was calculated as an average of the gauges in the "S1" position on the left and right side of the girder:

$$\varepsilon_x = \frac{\varepsilon_{S1L} + \varepsilon_{S1R}}{2}$$

COMPARISON BETWEEN FIELD TEST AND MODELING

The experimental field testing results are compared with the ones from the developed two models and presented below. Figure 16 shows the comparison between single lane moment distribution factors from field test data and ones from the models. And Figure 17 shows the shear distribution factors.

From these figures, we found the following single lane load distribution factors based on field testing results, as shown in Table 2.

Table 2 Average Distribution Factors (DF) from Field Tests of Set 1 Bridges

	Edge Girder	2nd Girder	Middle Girder
Moment DF	.446	.344	.278
Shear DF	.661	.439	.479

These distribution factors represent the fraction of load which a girder carried when the load vehicle drove directly over the top of that girder. These values are an average derived from data from two different methods of loading over both the north bound and south bound bridges.

Also from these figures, we found that 3D FE model predicts the distribution factors very well while two grillage models produce a little higher distribution factors. The calibrated 3D FE model can be used to study shear connectors and intermediate steel diaphragms because the hinge-connector elements produces connector forces directly instead of stresses and strains outputs. It is easier to build the 2D grillage model than to build the 3D FE model. The former outputs shear and moment forces directly while the later only gives girder strain values. In more details, Grillage Model 1 predicts midspan moment distribution factors better than Grillage Model 2 does, while the later predicts better shear distribution factors. The difference between the two models is the stiffness of the transverse beams in the grillage model.

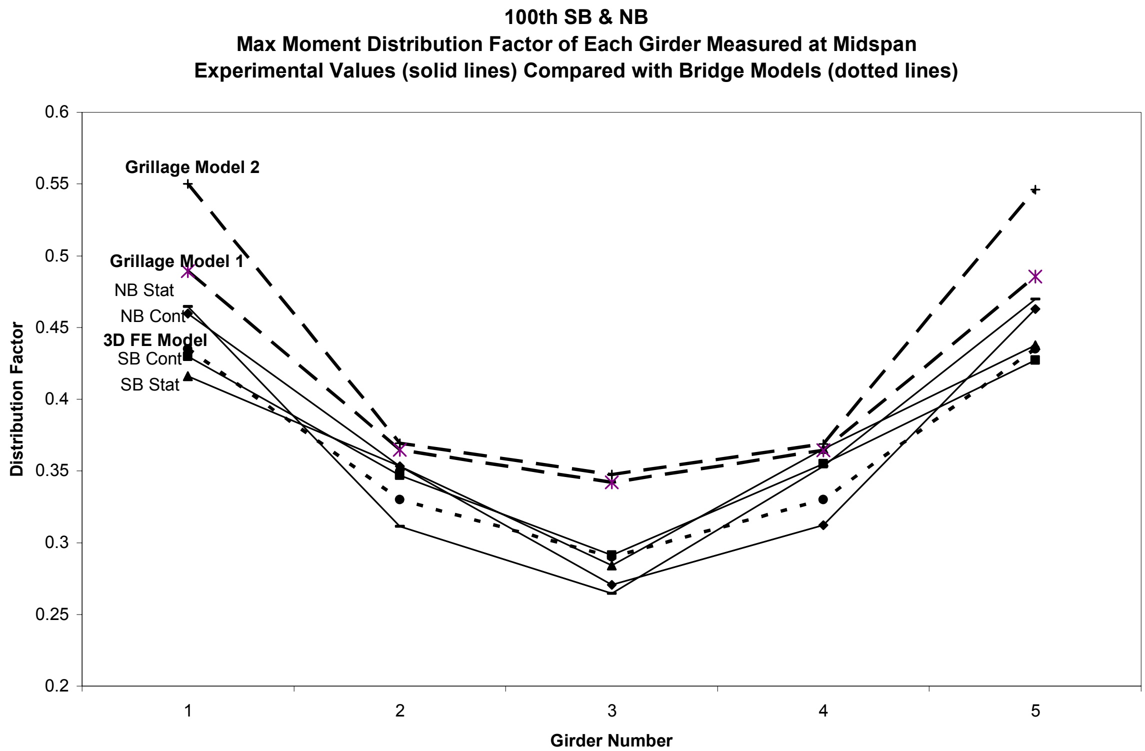

Fig. 16 Comparison of Moment Distribution Factors

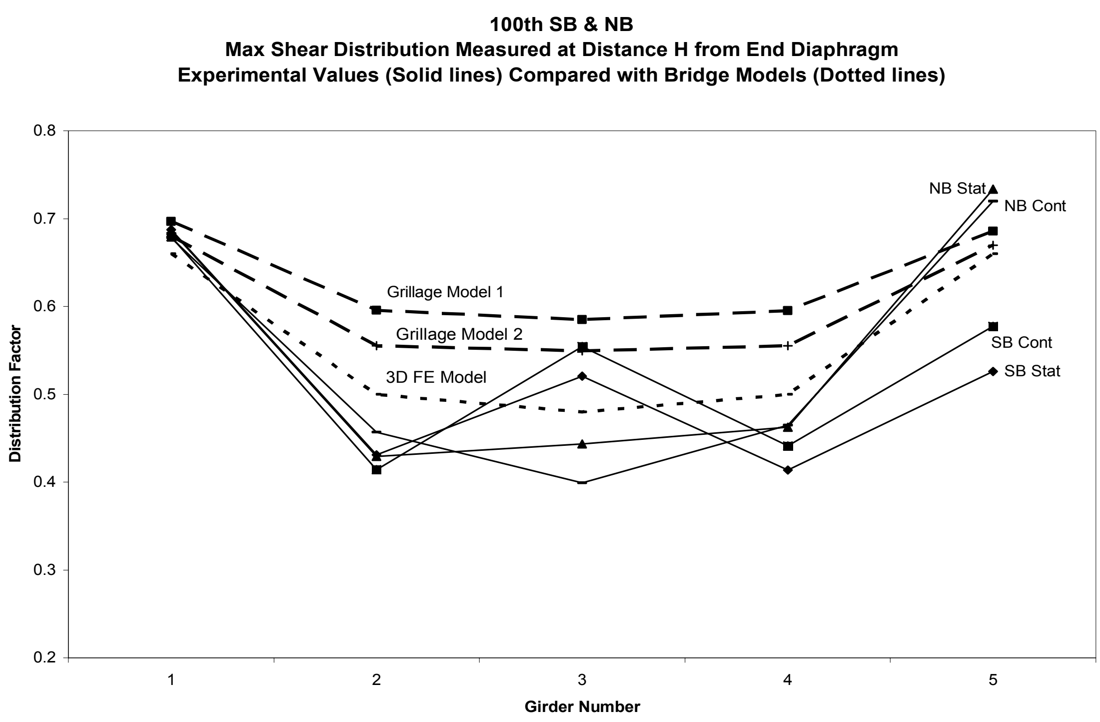

Fig. 17 Comparison of Shear Distribution Factors

COMPARISON WITH AASHTO LRFD SPECIFICATIONS

According to the current AASHTO LRFD Specifications, the decked bulb-tee girder bridges are categorized as "Precast Concrete Tee Section with Shear Keys **without** Transverse Post-tensioning." The load distribution factor equation for this type of bridges in LRFD Specifications can be compared with field testing as well as modeling results.

Figures 18 and 19 compare moment and shear distribution factors from field testing data with the DF equations predictions using AASHTO Specifications. The moment DF values from AASHTO LRFD are an average of 66% larger than the experimentally derived values and the shear DF values from AASHTO LRFD are an average of 26% larger than the experimental values.

For each of these graphs, the multiple presence factor was factored out for the AASHTO calculations so that the values would compare with the experimentally found values. DF values from a grillage model are also shown in the figures.

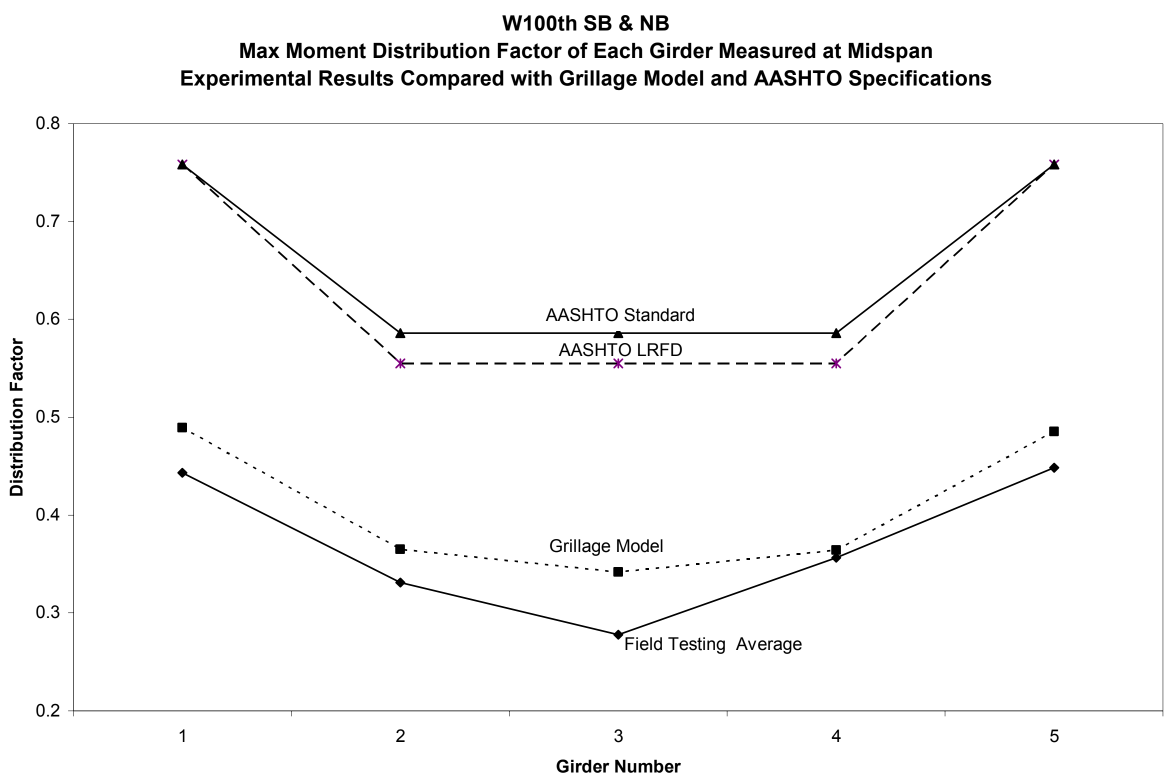

Fig. 18 Moment DF Comparison with AASHTO Specifications

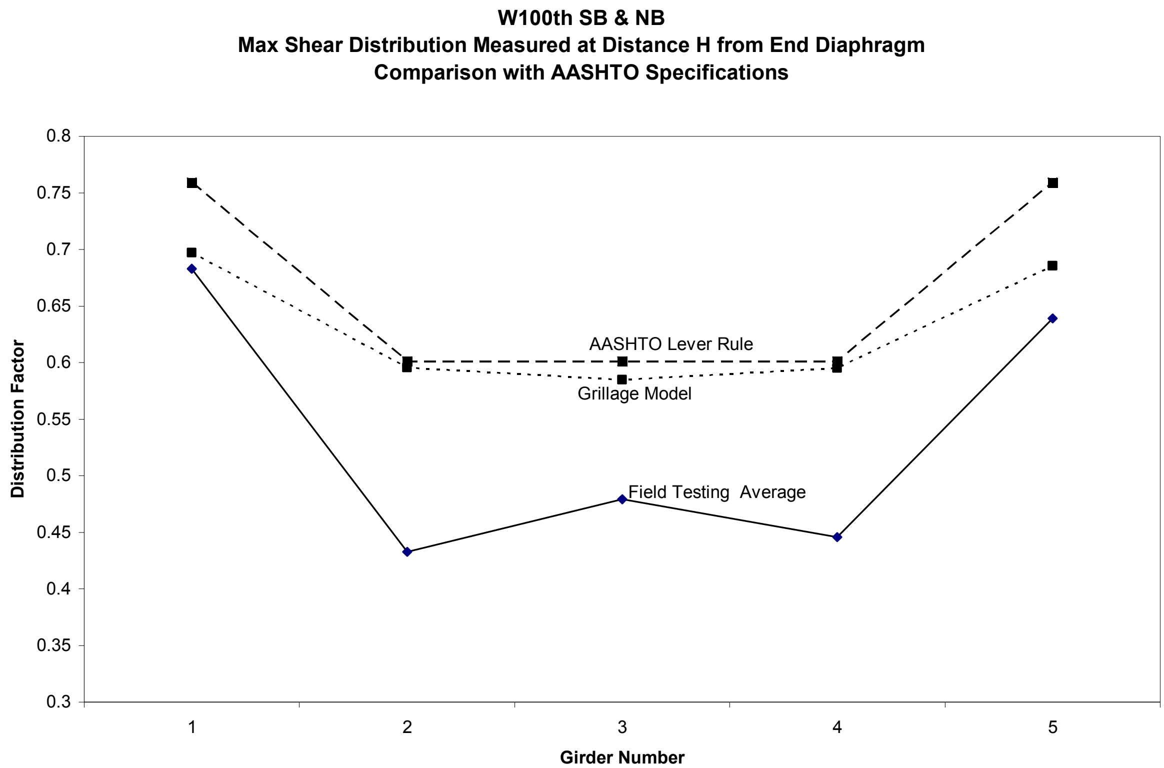

Fig. 19 Shear DF Comparison with AASHTO Specifications

When the DF values are calculated using the AASHTO LRFD equations for the "Precast Concrete Tee Section with Shear Keys **with** Transverse Post-tensioning," there is a much closer comparison with experimental data. As shown in Figure 20, the moment DF values are only 5% larger than the experimental values for the interior girders. However, the exterior girders which still use the lever rule to determine the distribution factor give values that are 70% higher than the experimental values. As shown in Figure 21, the shear DF values are 20% larger than the experimental values. As expected, Figure 22 shows the concrete strength has no impact on DF values.

CONCLUSIONS

Based on field tests and analyses of two models, the following conclusions are made:

(1) From the comparison of the model predictions with field testing results of W100th Ave bridges, the developed 3D FE model and 2D grillage model work well in predicting the single lane live load distribution factors;
(2) The moment DF values from AASHTO LRFD are an average of 66% larger than the experimentally derived values and the shear DF values from AASHTO LRFD are an average of 26% larger than the experimental values;

(3) The field testing data collected from the twin bridges at W100th Ave shows that the AASHTO equations when applied to these bridges are excessively conservative for the single lane loaded condition. The data is much more closely approximated by the single lane DF equations in AASHTO LRFD Specifications reserved for decked bulb-tee girder bridge systems that have transverse post-tensioning to act as a single unit;

(4) When comparing with field testing results, 3D FE model gives a closer prediction than 2D grillage models. Since the hinge-connector elements in 3D FE model output connector forces directly, the calibrated 3D FE model can be used to study the shear connectors in decked bulb-tee bridges;

(5) The stiffness modelling of the transverse beams play a significant role in the accuracy of the grillage models. Grillage models show that the concrete strength has no impact on DF values.

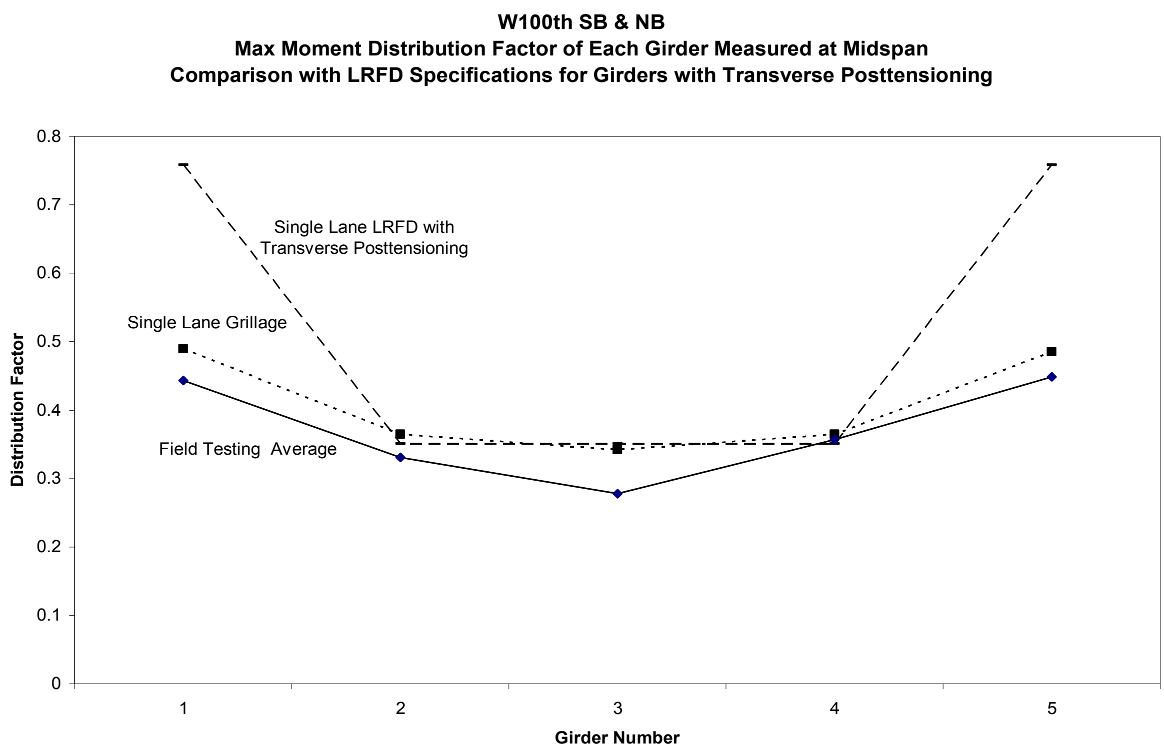

Fig. 20 Moment DFs Comparison

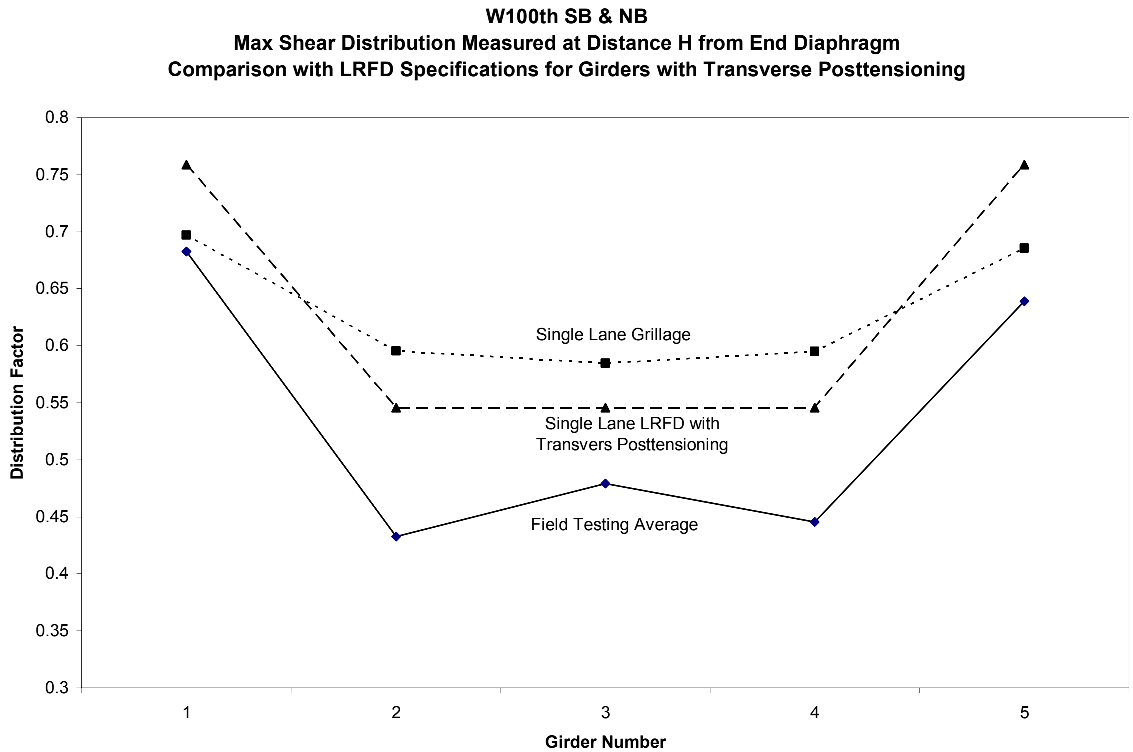

Fig. 21 Shear DFs Comparison

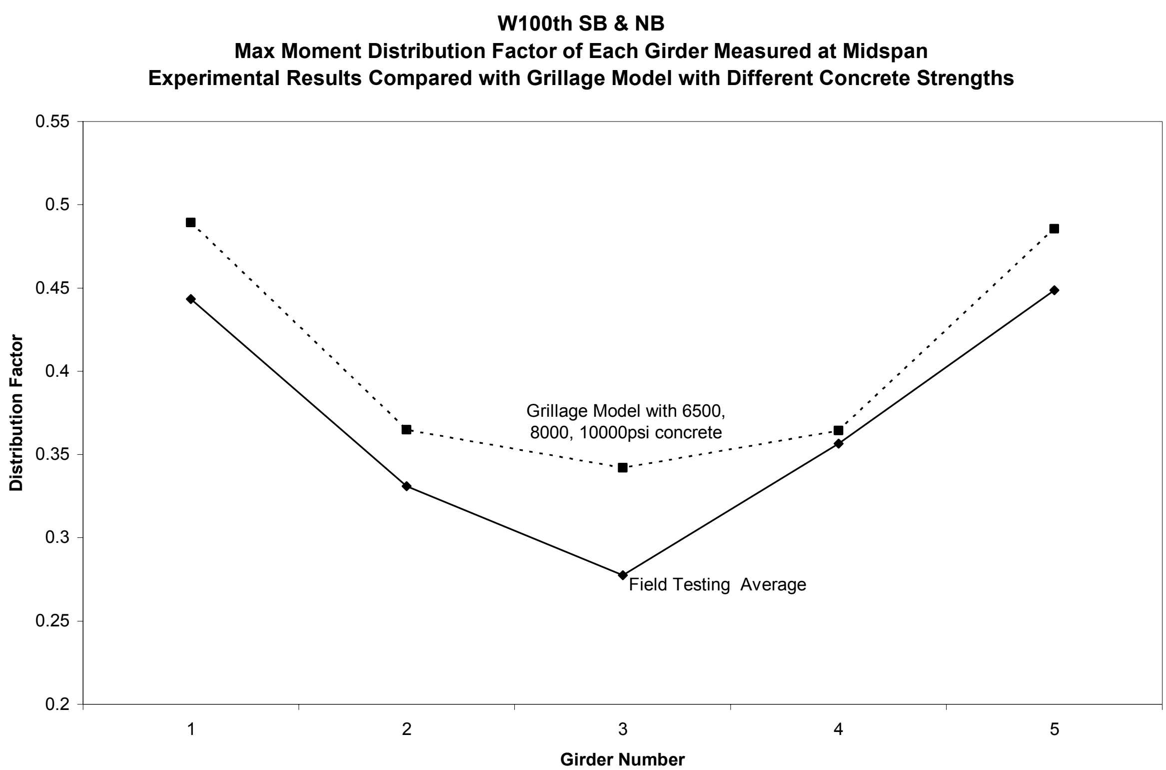

Fig. 22 Impact of Concrete Strength on DFs

ACKNOWLEDGEMENT

This research project is funded by the Alaska Department of Transportation and Public Facilities (AKDOT&PF) and FHWA. From AKDOT&PF Bridge Section, Gary Scarborough and John Orbistondo assisted in the field testing.

REFERENCES

1. "LRFD Bridge Design Specifications," American Association of State Highway and Transportation Officials, Inc., Second Edition, 1998.
2. Ma, Z. (J.), Hulsey, J. L., Millam, J., and Chaudhury, S., "A Note on Single Lane Live Load Distribution Factors for the Alaska Style Bulb-Tee Bridges," Proceedings of the First National Bridge Conference, October 6-9, 2002, Nashville, Tenn.
3. Sanders, W. W. and Elleby, H. A., "Distribution of Wheel Loads on Highway Bridges," NCHRP Report 83, Highway Research Board, 1970.
4. Stanton, J. and Mattock, A. H., "Load Distribution and Connection Design for Precast Stemmed Multibeam Bridge Superstructures," NCHRP Report 287, Nov., 1986.
5. "Standard Specifications for Highway Bridges," American Association of State Highway and Transportation Officials, Inc., 17th Edition, 2002.
6. "AASHO Road Test Report 4: Bridge Research," HRB Spec. Rep. 61D, 1962.
7. Bramer, C. R., Uyanik, M. E., and Moreadith, F. L., "Prestressed Concrete Channel Bridges for Secondary Roads: An Investigation of the Elastic Load Distribution Under Live Loading." Engineering Research Department Report ERD-110-E, North Carolina State University, 1962.
8. Rowe, R. E., "Loading Tests on Langstone Bridge, Hayling Island, Hampshire," Cement and Concrete Assn. Tech. Rep. TRA/289, 1958.
9. Rowe, R. E., "Loading Tests on Two Prestressed Concrete Highway Bridges," Inst. Civil Eng. Proc., 13, 1959.
10. Zokaie, T., Osterkamp, T. A., and Imbsen, R. A., "Distribution of Wheel Loads on Highway Bridges," Final Report, V. 1 and 2, prepared for NCHRP, Transportation Research Board, National Research Council, Washington D. C., 1991.
11. Imbsen, R. A. and Nutt, R. V., "Load Distribution Study on Highway Bridges Using STRUDL Finite Element Analysis Capabilities," First Conference on Computing in Civil Engineering, Atlanta, Ga., June 1978.
12. Hays, C. O., Sessions, L. M., and Berry, A. J., "Further Studies on Lateral Load Distribution Using Finite Element Methods." Transportation Research Record, (1072). Transportation Research Board, Washington, D. C., p6-14, 1986.